Spatial scales of climate response to inhomogeneous radiative forcing

Drew Shindell, Michael Schulz, Yi Ming, Toshihiko Takemura, Greg Faluvegi, V. Ramaswamy

▶ **To cite this version:**

Drew Shindell, Michael Schulz, Yi Ming, Toshihiko Takemura, Greg Faluvegi, et al.. Spatial scales of climate response to inhomogeneous radiative forcing. Journal of Geophysical Research, 2010, 115 (D19), 10.1029/2010JD014108 . hal-03201079

HAL Id: hal-03201079
https://hal.science/hal-03201079

Submitted on 18 Apr 2021

HAL is a multi-disciplinary open access archive for the deposit and dissemination of scientific research documents, whether they are published or not. The documents may come from teaching and research institutions in France or abroad, or from public or private research centers.

L'archive ouverte pluridisciplinaire **HAL**, est destinée au dépôt et à la diffusion de documents scientifiques de niveau recherche, publiés ou non, émanant des établissements d'enseignement et de recherche français ou étrangers, des laboratoires publics ou privés.

Spatial scales of climate response to inhomogeneous radiative forcing

Drew Shindell,[1] Michael Schulz,[2] Yi Ming,[3] Toshihiko Takemura,[4] Greg Faluvegi,[1] and V. Ramaswamy[3]

Received 26 February 2010; revised 6 May 2010; accepted 24 May 2010; published 7 October 2010.

[1] The distances over which localized radiative forcing influences surface temperature have not been well characterized. We present a general methodology to analyze the spatial scales of the forcing/response relationship and apply it to simulations of historical aerosol forcing and response in four climate models. We find that the surface temperature response is not strongly sensitive to the longitude of forcing but is fairly sensitive to latitude. Surface temperature responses in the Arctic and the Southern Hemisphere extratropics, where forcing was small, show little relationship to local forcing. Restricting the analysis to 30°S–60°N, where nearly all the forcing was applied, shows that forcing strongly influences response out to ~4500 km away examining all directions. The meridional length of influence is somewhat shorter (~3500 km or 30°), while it extends out to at least 12,000 km in the zonal direction. Substantial divergences between the models are seen over the oceans, whose physical representations differ greatly among the models. Length scales are quite consistent over 30°S–60°N land areas, however, despite differences in both the forcing applied and the physics of the models themselves. The results suggest that better understanding of regionally inhomogeneous radiative forcing would lead to improved projections of regional climate change over land areas. They also provide quantitative estimates of the spatial extent of the climate impacts of pollutants, which can extend thousands of kilometers beyond polluted areas, especially in the zonal direction.

Citation: Shindell, D., M. Schulz, Y. Ming, T. Takemura, G. Faluvegi, and V. Ramaswamy (2010), Spatial scales of climate response to inhomogeneous radiative forcing, *J. Geophys. Res.*, *115*, D19110, doi:10.1029/2010JD014108.

1. Introduction

[2] Given the complexity of the Earth's climate system, it is exceedingly difficult to understand cause and effect from observations. Climate models contain representations of our best current understanding of physical processes at large scales, so are used in combination with observations to unravel how changes in the Earth's energy balance with space (radiative forcing) lead to climate change at the surface. Although models are an ideal tool for examining cause and effect, nonetheless, it remains problematic to understand many issues in the extremely complex global climate models currently in use. For example, while the impact of globally quasi-uniform forcings such as that due to increased atmospheric CO_2 is relatively straightforward to study, the response to regionally inhomogeneous forcings is more challenging. As both the atmosphere and ocean transport heat and energy, the impact of localized forcing might logically be assumed to depend upon the strength and direction of local circulation as well as local climate feedbacks. In principle, the simplest approach to characterizing this dependence is to perform thousands of experiments, each of which changes forcing in one place at a time, and evaluate the response. This is conceptually similar to evaluating the Green's function for the response to forcing at each point and assuming linearity in the overall response to forcing at many locations. While there may be some justification for that assumption and while it could provide useful insights [*North et al.*, 1992], such an approach is both prohibitively expensive computationally and would also require unrealistically large forcing to induce a response that would be discernable over internal variability in a realistic climate model.

[3] An alternative is to examine simulations in which forcing was applied inhomogeneously but in many locations at once (e.g., historical or projected changes in aerosols and/or ozone with time). Early studies of the impact of regionally inhomogeneous radiative forcing using this approach showed that the climate response was not necessarily collocated with the forcing [*Mitchell et al.*, 1995;

[1]NASA Goddard Institute for Space Studies, New York, New York, USA.
[2]Laboratoire des Sciences du Climat et de l'Environnement, Commissariat à l'Energie Atomique/CNRS-Institut Pierre-Simon Laplace, Gif-sur-Yvette, France.
[3]NOAA Geophysical Fluid Dynamics Laboratory, Princeton, New Jersey, USA.
[4]Research Institute for Applied Mechanics, Kyushu University, Fukuoka, Japan.

Copyright 2010 by the American Geophysical Union.
0148-0227/10/2010JD014108

Table 1. Model Configurations, Forcing, and Response[a]

	GFDL	SPRINTARS	IPSL	GISS
Resolution	2 × 2.5	2.8 × 2.8	2.8 × 3.8	4 × 5
Aerosols	Direct + indirect	Direct + indirect	Direct + indirect, reflective only	Direct + indirect
Ocean	Mixed-layer	Mixed-layer	Dynamic	Dynamic
Radiative forcing (W/m^2)	−2.13	−0.86	−0.69	−1.01
Surface temperature change (C)	−1.92	−0.87	−0.61	−0.49
Reference for aerosol driven climate simulations	*Ming and Ramaswamy* [2009]	*Takemura et al.* [2006]	*Dufresne et al.* [2005], *Hourdin et al.* [2006]	*Hansen et al.* [2007]

[a]Radiative forcing (at the tropopause) and surface air temperature are global mean annual average changes for the present-day relative to the preindustrial. Resolution is horizontal degrees (latitude × longitude).

Taylor and Penner, 1994]. A substantial body of more recent work not only supports that conclusion but also indicates that regional forcing from ozone and aerosols can have an important impact on regional climate change distinct from that of quasi-uniform forcings [*Berntsen et al.*, 2005; *Boer and Yu*, 2003; *Chung and Seinfeld*, 2005; *Feichter et al.*, 2004; *Hansen et al.*, 2005; *Jacobson*, 2002; *Levy et al.*, 2008; *Roberts and Jones*, 2004; *Shindell*, 2007; *Shindell and Faluvegi*, 2009; *Shindell et al.*, 2008; *Stier et al.*, 2006]. These studies typically examined the response to aerosol forcing. However, as aerosols were changed over many parts of the globe simultaneously, as in the earlier studies, they do not clearly relate climate response to forcing at a particular location. Two studies examined the response to aerosol forcing in particular latitude bands or areas [*Chou et al.*, 2005; *Shindell and Faluvegi*, 2009]. Both studies indicated that climate responses could extend well beyond the forcing location but did not attempt to quantify those length scales. Hence, the spatial relationship between forcing and response remains poorly quantified. Here we present a new approach to analyzing this relationship and examine multiple models to better characterize the robustness of our conclusions.

2. Simulations

[4] We perform analysis of four general circulation models (GCMs) that simulated the preindustrial (1871–1890) to present-day (1981–2000) radiative forcing due to aerosols and the response to that aerosol radiative forcing in a coupled ocean-atmosphere configuration. The models are those developed by the NASA Goddard Institute for Space Studies (GISS); the University of Tokyo, National Institute for Environmental Studies and Frontier Research Center for Global Change (the Model for Interdisciplinary Research On Climate (MIROC) GCM and Spectral Radiation-Transport Model for Aerosol Species (SPRINTARS) aerosol model); the Institute Pierre Simon Laplace (IPSL); and the NOAA Geophysical Fluid Dynamics Laboratory (GFDL). For GISS, IPSL, and SPRINTARS, the aerosol forcings are those used in the groups' Intergovernmental Panel on Climate Change Fourth Assessment Report (AR4) simulations (Table 1). For GFDL, results are from a slightly newer model including prognostic aerosol indirect effects. For GISS and IPSL, simulations are those performed as additional runs for AR4 separating aerosols and other forcings (and thus using the identical models). For SPRINTARS and GFDL, these were simulations using mixed-layer ocean models performed as separate studies to examine the response to aerosols. Further details on the climate models and aerosol simulations are given in the references provided in Table 1. As we focus on the relationship between forcing and response, most specific details on how the forcing was generated are not of great importance (including the fact that the global mean annual average forcing differs by a factor of 3). The models generally include similar physical processes that affect the climate, although of course, the way these are represented varies across models, with the notable exception of ocean dynamics as mentioned above. Spatial maps of radiative forcing and surface temperature response (Figure 1) are the primary model output we use to analyze the forcing/response relationship.

3. Analysis Methodology

[5] The model fields (Figure 1) show that while there is clearly some association between the locations of forcing and surface temperature responses, there is obviously not a one-to-one mapping of response onto forcing. For example, the very large negative forcings over industrialized areas often do not induce a concomitantly large cooling in those regions, while positive forcing over North Africa and the Arabian Peninsula in the three models with absorbing aerosols does not lead to warming in those regions. Additionally, we see that cooling is generally at or near its maximum in the Arctic even though the negative forcing peaks at Northern midlatitudes.

[6] After exploring several potential methods, we have concluded that aspects of the forcing/response relationship can be discerned by analysis of the spatial autocorrelation (circular, meridional, or zonal) of the forcing and response patterns for each model calculated as a function of distance. For circular spatial autocorrelation, each grid point value is related to the mean value on circles around this grid point. The circles for a given characteristic radius (= distance) are established such that they are equal area circles on the sphere around all grid points. Autocorrelations are calculated after removing the mean and normalizing the field by its standard deviation to better discern spatial variations. We examine the enhanced autocorrelation of the response field $f2$ relative to the input field $f1$: enhanced_autocorrelation ($f2$ versus $f1$) = autocorrelation ($f2$) − autocorrelation ($f1$). An enhancement in autocorrelation of the response relative to the forcing is indicative of smoothing in the response relative to the input driving forcing field. The distance over which the enhancement takes place thus provides a characteristic radius of influence length scale for the

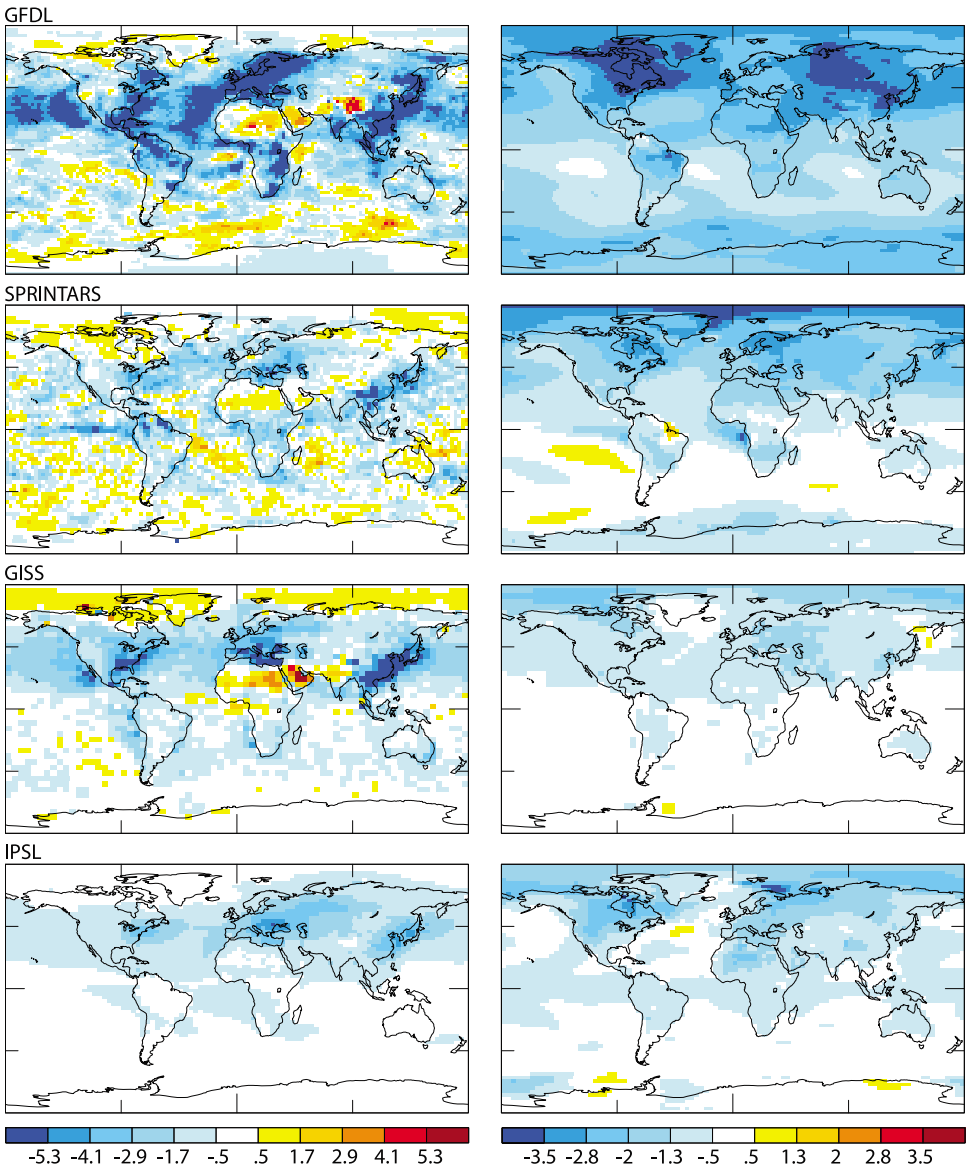

Figure 1. (left) Instantaneous tropopause aerosol radiative forcing (W/m^2) and (right) the resulting surface temperature change (°C) in the four climate models. Values are annual mean preindustrial to present-day changes.

forcing/response relationship. To demonstrate the utility of this methodology, we look first at the comparatively simple case of carbon monoxide (CO) emissions and concentrations as simulated in the GISS model as an example. CO is emitted at the Earth's surface and is also both chemically created and removed in the atmosphere. It has a lifetime on the order of 1–2 months in the free troposphere, allowing it to be spread by atmospheric circulation fairly broadly but not so broadly as to lose all spatial structure, making it ideal for our purposes.

[7] Surface level CO is smoother than the underlying emissions distribution, but it retains a great deal of the spatial pattern of the highly localized emission sources with clear local maxima in high-emitting regions (Figure 2). In contrast, midtropospheric CO is greatly smoothed relative to the emissions, although there are nonetheless clear maxima related to tropical biomass burning regions and greater concentrations in the Northern Hemisphere extratropics than at other latitudes. We first examine the enhancement of the spatial autocorrelation of the concentrations relative to the emissions for CO over all angles (which we term circular analysis). This enhanced autocorrelation is simply the difference between the single-field autocorrelations shown in Figure 2. We see that globally the surface layer concentrations have an enhanced autocorrelation relative to the emissions that is greatest at very small spatial scales of ~500 km (Figure 3, top left). Were the concentration and emission fields identical, their autocorrelations would of course be the same and hence there would be no enhancement. A positive value for the enhancement indicates that the surface layer concentrations are indeed smoothed relative to the input emissions, with the length scale of strong enhancement showing the radius over which the emissions have greatest influence on concentrations. Hence,

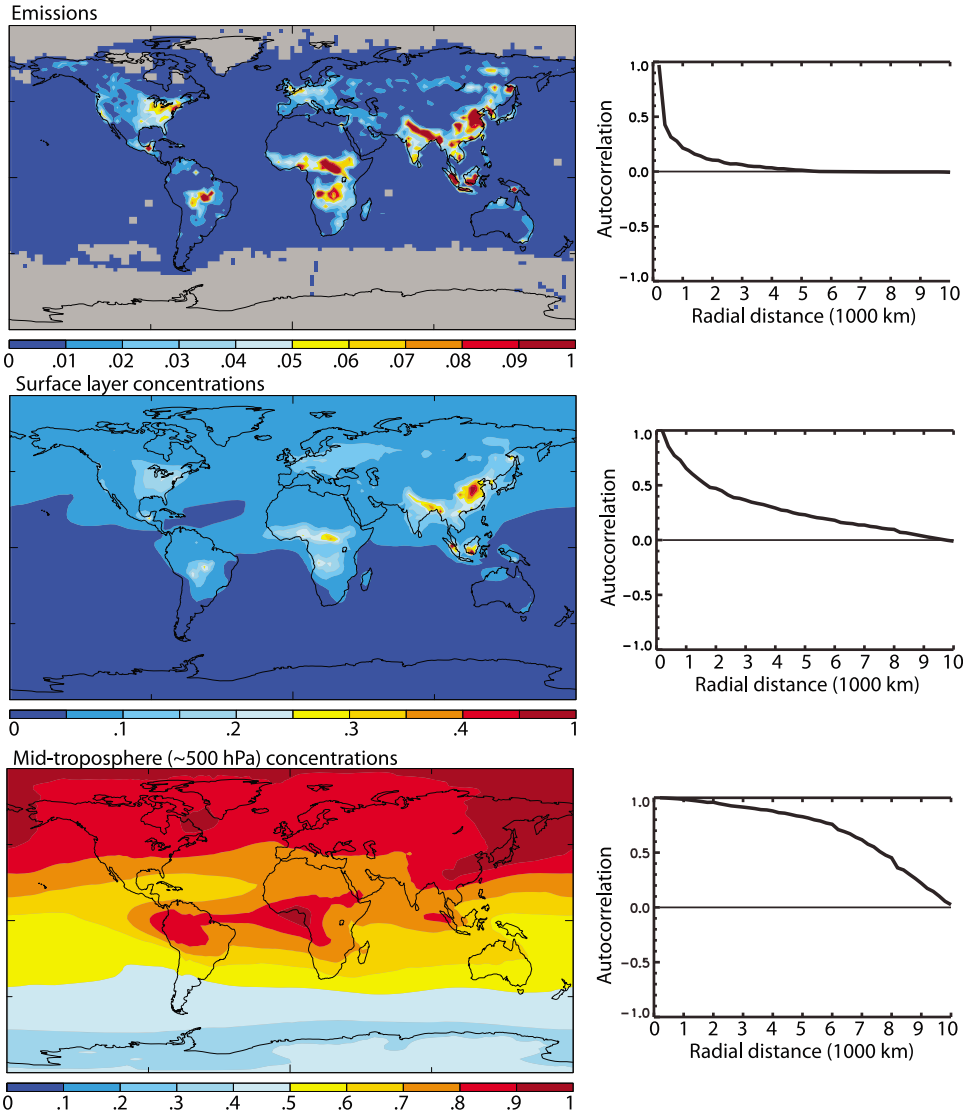

Figure 2. (top) CO emissions, (middle) surface level concentration, and (bottom) midtroposphere concentration (~500 hPa). (left) Maps, with all values normalized to the maximum in the field. (right) Spatial autocorrelations of each field (using circular analysis).

the influence of emissions on surface concentrations is greatest at the minimum distance that can be discerned and decreases steadily at longer distances. In contrast, the influence of surface emissions on midtropospheric concentrations takes place over a much broader area with a maximum increase in autocorrelation over radii of ~4000 km and a substantial effect out to ~8000 km. Note that the apparent increases in the enhanced autocorrelation at very short length scales do not represent growing influence over these scales, but reflect the enhancement limit created by differencing with respect to the input field, as the latter is large at very short scales.

[8] By calculating the autocorrelations exclusively as a function of distance in either the meridional or zonal direction rather than using circular analysis, we can learn even more about how the concentrations relate spatially to the emissions. For both atmospheric layers, the autocorrelations show a much more rapid drop off in enhancement for meridional calculations than zonal calculations, indicating that the north-south distance over which the emissions strongly influence the concentrations is substantially less than the east-west distance. In both cases, meridional influences are greatest for distances less than 2000 km and extend out to only about 4000–5000 km, while in the zonal direction influence is large even out to distances of 10,000 km or more (though it peaks at distances out to ~5000–6000 km in the midtroposphere and ~500 km at the surface). Performing the same analysis with black carbon (BC) rather than CO demonstrates that the enhanced correlation measure is clearly able to represent the difference between these two species, showing shorter length scales for the relationship between BC emissions and concentrations than for CO, consistent with the lifetime of BC being ~1 week, whereas the lifetime of CO is ~1–2 months. Negative enhancements in autocorrelation in the meridional direction are a result of the large-scale structure that extends from pole to pole in the midtroposphere for CO (Figure 2) and also for BC as its lifetime is considerably longer in the midtroposphere. This

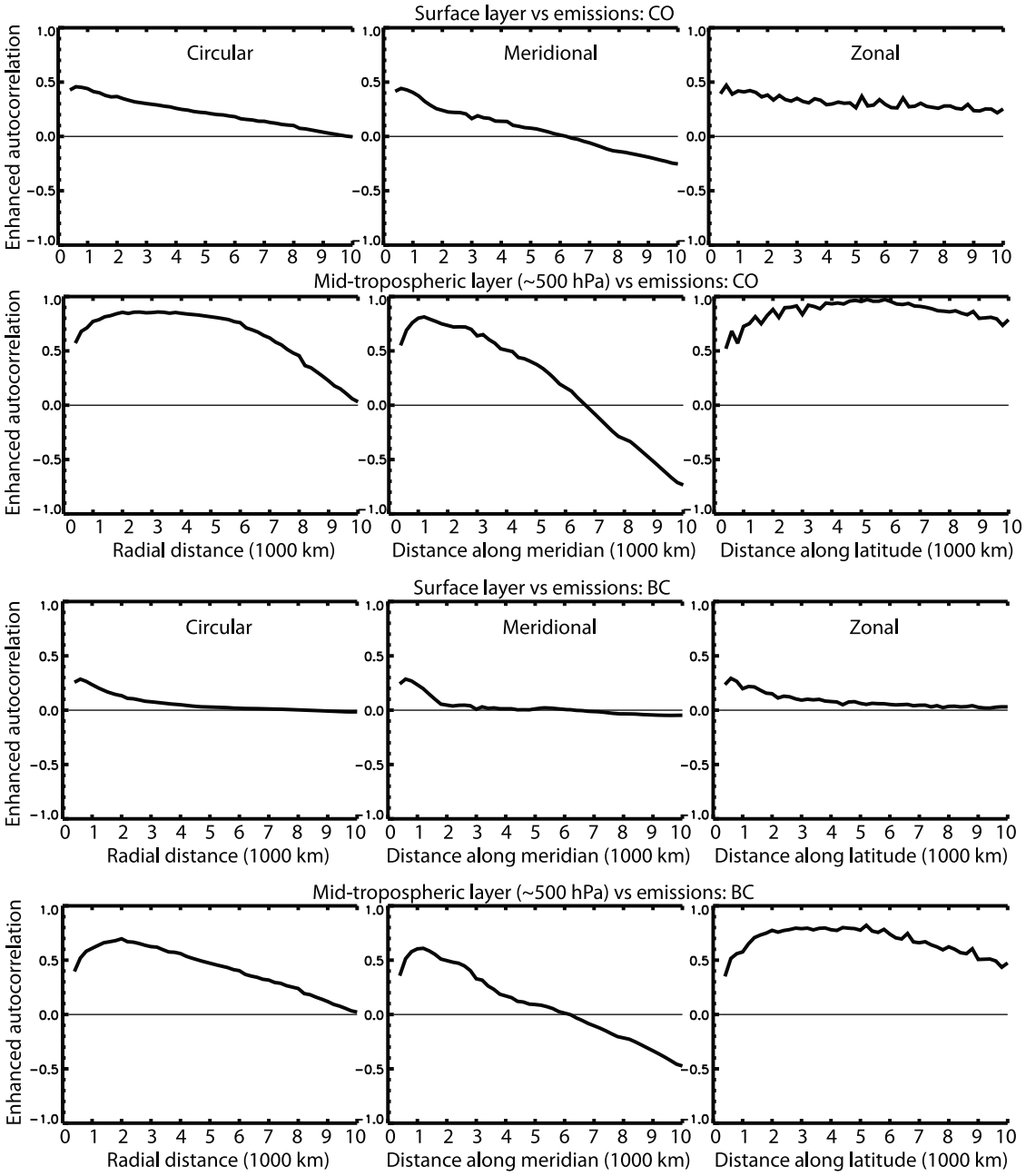

Figure 3. Enhancement of spatial autocorrelation of atmospheric concentrations relative to surface emissions for (top) CO and (bottom) BC in the GISS model as an illustrative example. Atmospheric concentrations are at the indicated layers for (left) circular autocorrelations, (middle) autocorrelations calculated only in the meridional direction, and (right) autocorrelations calculated only in the zonal direction. Values at distances less than a single model grid box are by definition zero and hence are not shown.

meridional gradient leads to lower spatial autocorrelation in the concentrations than in the emissions at long distances, as the emissions field is fairly uniform, with virtually no emissions, over areas away from major source regions, whereas the midtropospheric concentrations, once the mean is removed, show a pronounced anticorrelation in the meridional direction. This makes intuitive sense as the difference in concentration between two distant points at the same longitude are in general not strongly related to emissions at that particular longitude but generally reflect the total emissions in each hemisphere.

[9] These analyses of CO are all qualitatively consistent with what one would estimate from simply examining the spatial patterns of the emissions and concentrations (Figure 2) and are all in agreement with our understanding of atmospheric processes. For example, constituent transport is more rapid in the zonal direction than the meridional; hence, length scales of influence are much longer in that direction. Similarly, CO in the midtroposphere (and the free troposphere in general) is much more well-mixed than CO near the surface, leading to longer length scales aloft relative to those at the surface. What the method gives us is the ability

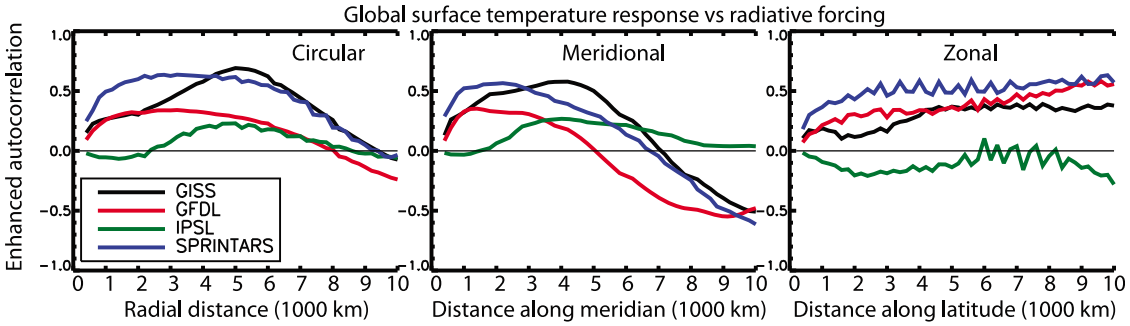

Figure 4. Enhancement of spatial autocorrelation of surface temperature changes relative to radiative forcing in the four indicated GCMs for aerosol forcing/response simulations. Results are shown for (left) circular autocorrelations, (middle) autocorrelations calculated only in the meridional direction, and (right) autocorrelations calculated only in the zonal direction as in Figure 3.

to quantify the spatial relationships between an input driving field (CO emissions in this example) and the response field (CO concentrations), and this example shows that the method provides sensible results that are consistent with the way atmospheric physics and chemistry are known to work. Similarly, length scales for BC are substantially shorter than those for CO, and in particular, the ~1 week lifetime leads to very short length scales (~1500 km) near the surface in both the zonal and meridional directions, whereas BC that reaches the midtroposphere is able to be transported longer distances but still less than those for CO, as expected. We believe that these examples demonstrate that our metric provides useful insight into the spatial relationship between driver and response fields.

4. Climate Forcing and Response Results

[10] We now turn to the more complex case of the physics of the climate system by using radiative forcing as the input driving field and surface temperature change as the response. We examine the enhanced autocorrelation in the surface temperature response to radiative forcing from aerosols relative to the input radiative forcing in the four GCMs (Figure 4). The results using circular analysis suggest that globally, the forcing influences the response out to a characteristic distance of about 6000–7000 km, with substantial differences between the models. The analyses separating the two directions show that the length scale arises primarily from the meridional direction. That is, local temperatures are sensitive to forcing at latitudes within ~4000–6000 km distance (depending on the model, equivalent to ~35°–50°). In contrast, autocorrelation enhancements generally increase steadily with greater distance in the zonal direction, suggesting that responses are broadly sensitive to forcing at a given latitude regardless of the longitude at which the forcing is imposed. Note however that the zonal direction correlation enhancements do typically decrease past ~12,000 km (not shown), perhaps indicating that differences between land and ocean responses fundamentally limit the smoothing of the response in the zonal direction at these large length scales (i.e., the greater thermal inertia in the three ocean basins imposes a zonal asymmetry at roughly one third the global circumference even though the forcing may influence response across ocean basins).

[11] We note that the IPSL model, without absorbing aerosols and with little forcing over the oceans, has a much more spatially uniform radiative forcing than the other models (Figure 1). The autocorrelation of the forcing is thus substantially higher than in the other models out to ~3000 km in the meridional or circular analyses and at all length scales in the zonal analysis, whereas the autocorrelation of the response is sometimes slightly lower (especially in the zonal direction) but overall quite similar to that of the other models (Figure 5). Hence, the very small enhancements seen for small distances in the meridional case and at all lengths in the zonal case for this model appear to reflect our limited ability to discern the forcing/response relationship in those results because of the very

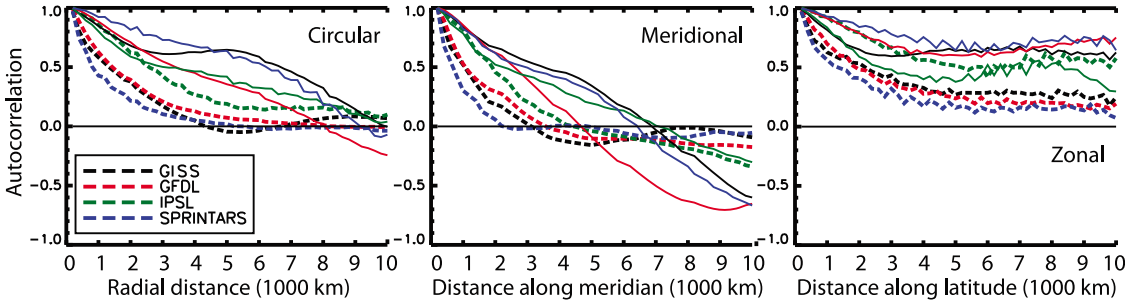

Figure 5. Spatial autocorrelations of the individual components (radiative forcing as heavy dashed lines; surface temperature response as light solid lines) used in the global enhancement (response minus forcing) calculations shown in Figure 4.

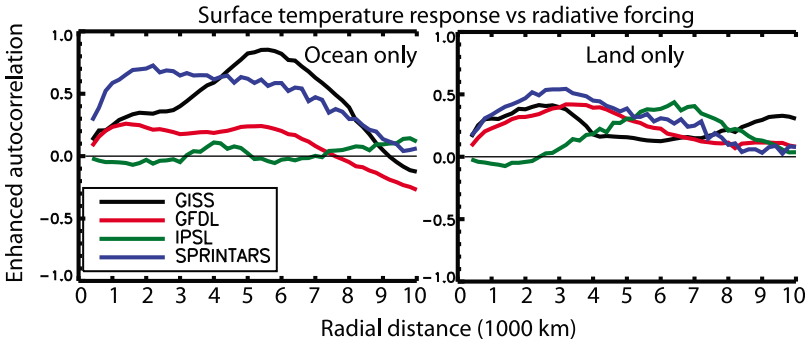

Figure 6. Enhancement of spatial autocorrelation of surface temperature changes relative to radiative forcing as in Figure 4 but separately for (left) ocean points and (right) land points using circular autocorrelations. The land area analysis excludes Antarctica.

homogeneous forcing rather than indicating a fundamental difference in this model's behavior.

[12] We can try to understand the source of the differences between the models by restricting the analysis to either ocean or land areas. We find that the autocorrelation enhancement is rather different for these two regions (Figure 6). In particular, there is much greater divergence between models over the oceans. Returning to the input forcings and responses, we see that for the GISS and IPSL models, the ocean response is generally rather weak and uniform (Figure 1). Hence, for the IPSL model, with little structure in the ocean forcing, both the response and forcing have high autocorrelations and hence the enhancement is near zero at all length scales (this could result at least partially from strong oceanic mixing as well). For the GISS model, the response appears to integrate forcing over large areas with maximum relative smoothing at radii of around 4500–7000 km, consistent with the general impression that the oceanic response remains quite smooth despite large-scale structure in the forcing (Figure 1). This suggests substantial mixing of the forced signal by this model's dynamic ocean. The GFDL model exhibits substantial inhomogeneity in both forcing and response, including over the oceans. In particular, the autocorrelation in surface temperature response in this model is substantially less than in the other three models, especially in the meridional direction (Figure 5). The lower autocorrelation in response results primarily from ocean areas, presumably indicating a more heterogeneous response in the mixed-layer ocean model used there relative to the dynamic ocean models. This leads to relatively low enhancement of the autocorrelation of response relative to forcing over the oceans at all length scales in this model (Figure 6), although there is clearly some influence of the forcing on the response out to ~6000 km. The SPRINTARS model, like GISS, shows substantial enhancement of the autocorrelation of the response relative to the forcing but at generally smaller spatial scales similar to those in the GFDL model. In SPRINTARS, while the oceanic temperature response is overall smooth relative to the forcing, there is still substantial structure. In some of those instances, e.g., in the tropical Pacific and Atlantic, the response appears to follow the forcing fairly closely, consistent with the strong sensitivity of the response to forcing at relatively small spatial scales over the oceans in this mixed-layer model.

[13] In contrast, model results over land areas are much more consistent. Other than the low values at small spatial scales for IPSL discussed previously, the influence of the forcing on the response shows a fairly similar dependence on distance in all four models (Figure 6). Hence, the primary differences in the shape of the global results (Figure 4) seem to be due to enhancement at long distances in the GISS model seem to be due to strong mixing/weak response of the dynamic ocean (as well as the suppression of enhancement at small spatial scales in IPSL because of high homogeneity in the input forcing and potentially strong mixing in that model's dynamic ocean as well). The magnitude of the enhancement in the global analysis is also clearly influenced by the behavior of the ocean, as evidenced by the lower values seen in enhancements over the oceans and in the global case for the GFDL and IPSL models, as discussed above.

[14] The most consistent results of all are obtained when the analysis is restricted to the area from 30°S to 60°N (Figure 7). This analysis leaves out the Arctic, where there is very little forcing and in any case the responses are clearly not related to the local forcing (Figure 1) and leaves out the Southern Hemisphere extratropics, where again there is minimal forcing in most of the models so that the relative autocorrelation of the forcing and response means little. In the 30°S–60°N region, where the response would thus be expected to be more closely related to the forcing, the model average Pearson's correlation coefficient is ~70% higher than the global value, but it is still very small (R^2 = 0.06) given the smoothing of response relative to forcing. This emphasizes the limitations of analyses using the direct spatial correlation between the forcing and response fields. Our enhanced autocorrelation, however, shows useful information, with three of the four models showing nearly identical distance of influence structures in this region. Examination of the separate autocorrelations of forcing and response shows that the weakly negative enhancement in the IPSL model is in this case due to both more homogeneous input forcing and weaker autocorrelation of the surface temperature response in that model relative to the other three. The latter seems to be due primarily to the inhomogeneity of the ocean response discussed previously, perhaps because the response itself is generally small in that model, and hence, even small inhomogeneity can reduce the autocorrelation substantially. Hence, the distinct IPSL results may again stem at least partially from the small amplitude

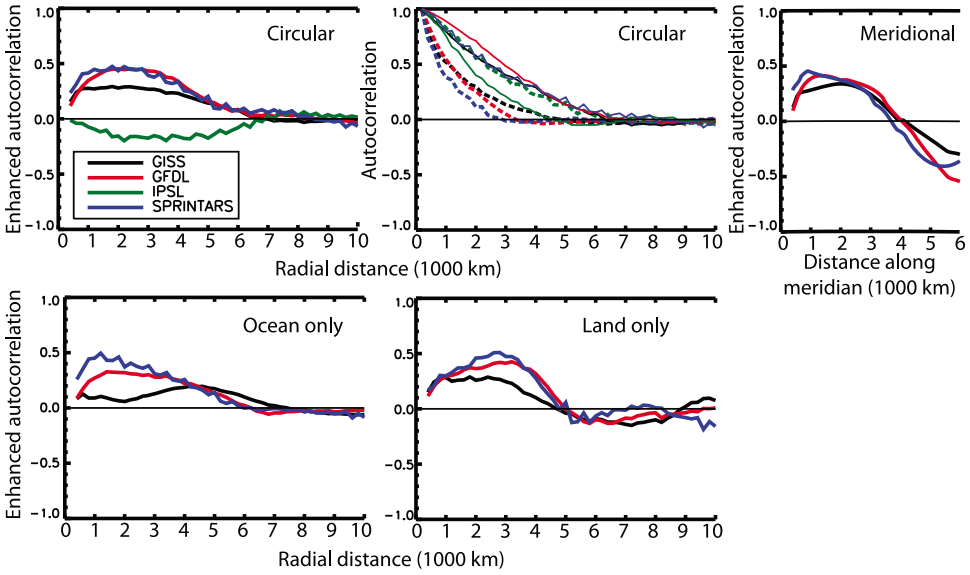

Figure 7. Analysis of spatial autocorrelations from 30°S to 60°N. Analyses show enhanced autocorrelation of surface temperature changes relative to radiative forcing using (top left) circular analysis over all points, (top middle) the individual component autocorrelations of radiative forcing (heavy dashed lines) and surface temperature response (light solid lines) for that analysis, and (top right) similar analysis of enhanced autocorrelation but in the meridional direction and (bottom) for circular analyses of ocean and land points separately. Note that autocorrelations of GISS and SPRINTARS responses in Figure 7 (top middle) are almost identical. The meridional analysis is truncated to 6000 km as the extent of the 30°S–60°N band is only 10,000 km.

signals seen in that model, and hence, we leave out that model for clarity in the few remaining analyses. The GFDL model has a more homogeneous response at spatial scales of 1000–3000 km than SPRINTARS, which stems largely from the smaller-scale structures apparent in the SPRINTARS response over the oceans. However, SPRINTARS also has a less homogeneous forcing, so that the enhancement is nearly identical, suggesting that despite real physical differences in forcing structure, length scales of response are robust across the models.

[15] Looking at the meridional direction autocorrelation enhancement for 30°S–60°N (Figure 7), we see even more consistent results for the three models. Forcing has a strong influence out to 3500 km in the meridional direction (30° latitude). At longer distances, the enhanced autocorrelation becomes negative, reflecting the limited meridional structure in radiative forcing at most longitudes compared with the strong meridional gradient in the surface temperature response between the hemispheres (Figure 1), as was also seen in midtropospheric CO versus CO emissions (Figures 2 and 3). The radius of influence extends out to ~5000–6000 km over the oceans but only ~4500 km over land. Again, influence extends further in the zonal direction but not as far in the meridional relative to these circular analyses. The ocean results again show a tendency to shorter length scales in the mixed-layer models, but results over land are quite consistent.

5. Discussion and Conclusion

[16] We believe that our method is generally applicable to diagnosing regional forcing and response relationships or indeed any spatial driver/response relationships, such as the emission/concentration relationships we used as examples. However, it is worth noting that the method has important limitations. While it characterizes length scales in the spatial structures in two fields and then compares them, it cannot reveal if the structures in the two fields are located in the same places. In our example of carbon monoxide, the colocation of emissions and surface concentration can clearly be seen, but it is less obvious for midtropospheric CO relative to emissions or for surface temperature change relative to radiative forcing. The equatorial Atlantic and East Pacific in SPRINTARS show clear colocation, but generally, this is not the case. As noted, the spatial correlation between radiative forcing and surface temperature in the four models is extremely small.

[17] Similarly, surface temperature response could occur via response of large-scale atmospheric or oceanic circulation, leading to particular length scales in the response that may not relate directly to the spatial pattern of the forcing. This may be at work in the ocean response in the models examined here, due to the different types of physics included, but appears to play a relatively minor role over land given the agreement between the models (though it might have larger effects in some regions during some seasons, e.g., in the Northern Hemisphere extratropics during winter when dynamics becomes relatively more important compared with radiation). This same difficulty in identifying dynamical signals precludes use of this method to investigate responses of climate parameters less closely tied to radiative forcing such as precipitation, which may also have distinct spatial patterns of response to inhomo-

geneous forcing [*Chou et al.*, 2005; *Kang et al.*, 2008; *Ming and Ramaswamy*, 2009].

[18] Despite these limitations, the agreement between three of the four models suggests that the length scale of influence of forcing, in areas where substantial forcing exists, may be a fairly robust feature across climate models, especially as there are good reasons to believe that the disagreeing model was simply not put to a sufficiently rigorous test to determine its distance of influence effectively. In this study, large variations in surface temperature responses over the ocean were the source of most differences between the models. Further work should include more models and especially models using various experimental setups that would allow us to test the apparent difference between mixed-layer and dynamic ocean models suggested by this study. For land areas, the responses of surface temperature were more consistent, suggesting that the response of atmospheric heat transport to regional forcing is probably fairly similar in the various models. Analysis of the area with substantial forcing, 30°S–60°N, shows very similar distances of influence in the models.

[19] In the general sense that the length scales over which forcing influences response are long, and hence, response is not colocated with forcing, our results are consistent with earlier studies. However, we do find distinct differences with respect to the response to forcing from well-mixed greenhouse gases in that the responses to inhomogeneous forcing extends only ~3500 km (30°) in the meridional direction. Hence, the response to aerosol or tropospheric ozone forcing can differ strongly from the response to well-mixed greenhouse gas forcing even though both may have comparable impacts on global mean temperatures. In fact, the spatial correlation between the surface temperature responses to aerosols and well-mixed greenhouse gases is only $R^2 = 0.45$ for land areas (0.32 without IPSL), indicating that the response to spatially varying forcing is not inhomogeneous simply because of geographic differences in climate feedbacks that respond to any forcing. Rather, the forcing tends to broadly follow the location at which it is imposed but extends over substantially larger areas than the forcing itself, especially in the zonal direction. These length scales appear broadly consistent with qualitative results from the European Centre/Hamburg model [*Chou et al.*, 2005] and the GISS model [*Shindell and Faluvegi*, 2009] in prior studies of the climate response to forcing imposed in discrete areas and are even of a similar order to the quantitative values seen in an early study using a much simpler model [*North et al.*, 1992].

[20] Our results indicate that the majority of historical aerosol forcing having occurred at Northern Hemisphere midlatitudes has had a distinct impact on historical temperature trends, as concluded in prior studies for hemispheric or regional scales [*Andronova and Schlesinger*, 2001; *Hegerl et al.*, 2007; *Santer et al.*, 1996; *Shindell and Faluvegi*, 2009]. They also suggest that the recent and projected continuation of the shift in emissions of ozone and aerosol precursor emissions from the Northern Hemisphere midlatitude developed nations to lower-latitude developing nations will have significant impacts on regional temperature trends at these latitudes. There are also likely to be substantial impacts on the Arctic. The climate response in that area clearly does not follow the local forcing for the historical case when local forcing was small (Figure 1), and the ~30° meridional influence of forcing means that Arctic temperatures are strongly influenced by Northern Hemisphere midlatitude forcings.

[21] There are several additional implications of our results. The issue of transboundary air pollution has received much attention for decades. Our results indicate that for one country or regions' air pollution to influence climate elsewhere does not require the pollution itself to be transported long distances as its influence can be felt more than 10,000 km away in the zonal direction. The study also suggests that understanding of historical and future regional climate change could be improved by better characterization of inhomogeneous forcing from aerosols and tropospheric ozone.

[22] **Acknowledgments.** We thank NASA's Modeling and Analysis Program for support and Gavin Schmidt for helpful discussion. IPSL model simulations could be accessed thanks to the IPSL infrastructure Pole de modelisation, led by Jean-Louis Dufresne and Pascale Braconnot. Analysis was also supported by the (EU-EUCAARI) project (contract 036833-2).

References

Andronova, N. G., and M. E. Schlesinger (2001), Objective estimation of the probability density function for climate sensitivity, *J. Geophys. Res.*, *106*(D19), 22,605–22,611, doi:10.1029/2000JD000259.

Berntsen, T. K., J. S. Fuglestvedt, M. M. Joshi, K. P. Shine, N. Stuber, M. Ponater, R. Sausen, D. A. Hauglustaine, and L. Li (2005), Response of climate to regional emissions of ozone precursors: Sensitivities and warming potentials, *Tellus, Ser. B*, *57*, 283–304.

Boer, G., and B. Yu (2003), Climate sensitivity and response, *Clim. Dyn.*, *20*, 415–429.

Chou, C., J. D. Neelin, U. Lohmann, and H. Feichter (2005), Local and remote impacts of aerosol climate forcing on tropical precipitation, *J. Clim.*, *18*, 4621–4636.

Chung, S. H., and J. Seinfeld (2005), Climate response of direct radiative forcing of anthropogenic black carbon, *J. Geophys. Res.*, *110*, D11102, doi:10.1029/2004JD005441.

Dufresne, J.-L., J. Quaas, O. Boucher, S. Denvil, and L. Fairhead (2005), Contrasts in the effects on climate of anthropogenic sulfate aerosols between the 20th and the 21st century, *Geophys. Res. Lett.*, *32*, L21703, doi:10.1029/2005GL023619.

Feichter, J., E. Roeckner, U. Lohmann, and B. Liepert (2004), Nonlinear aspects of the climate response to greenhouse gas and aerosol forcing, *J. Clim.*, *17*, 2384–2398.

Hansen, J., et al. (2005), Efficacy of climate forcings, *J. Geophys. Res.*, *110*, D18104, doi:10.1029/2005JD005776.

Hansen, J., et al. (2007), Climate simulations for 1880–2003 with GISS modelE, *Clim. Dyn.*, *29*, 661–696.

Hegerl, G. C., F. W. Zwiers, P. Braconnot, N. P. Gillett, Y. Luo, J. A. Marengo-Orsini, N. Nicholls, J. E. Penner, and P. A. Stott (2007), Understanding and attributing climate change, in *Intergovernmental Panel on Climate Change Fourth Assessment Report*, edited by S. Solomon, Cambridge, New York.

Hourdin, F., et al. (2006), The LMDZ4 general circulation model: Climate performance and sensitivity to parametrized physics with emphasis on tropical convection, *Clim. Dyn.*, *27*, 787–813.

Jacobson, M. Z. (2002), Control of fossil-fuel particulate black carbon and organic matter, possibly the most effective method of slowing global warming, *J. Geophys. Res.*, *107*(D19), 4410, doi:10.1029/2001JD001376.

Kang, S. M., I. M. Held, D. M. Frierson, and M. Zhao (2008), The response of the ITCZ to extratropical thermal forcing: Idealized slab-ocean experiments with a GCM, *J. Clim.*, *21*, 3521–3532.

Levy, H., M. D. Schwarzkopf, L. Horowitz, V. Ramaswamy, and K. L. Findell (2008), Strong sensitivity of late 21st century climate to projected changes in short-lived air pollutants, *J. Geophys. Res.*, *113*, D06102, doi:10.1029/2007JD009176.

Ming, Y., and V. Ramaswamy (2009), Nonlinear climate and hydrological responses to aerosol effects, *J. Clim.*, *22*, 1329–1339.

Mitchell, J. F. B., R. A. Davis, W. J. Ingram, and C. A. Senior (1995), On surface temperature, greenhouse gases, and aerosols: Models and observations, *J. Clim.*, *8*, 2364–2386.

North, G. R., K.-J. Yip, L.-Y. Leung, and R. M. Chervin (1992), Forced and free variations of the surface temperature field in a general circulation model, *J. Clim.*, *5*, 227–239.

Roberts, D. L., and A. Jones (2004), Climate sensitivity to black carbon aerosol from fossil fuel combustion, *J. Geophys. Res.*, *109*, D16202, doi:10.1029/2004JD004676.

Santer, B. D., et al. (1996), A search for human influences on the thermal structure of the atmosphere, *Nature*, *382*, 39–46.

Shindell, D. (2007), Local and remote contributions to Arctic warming, *Geophys. Res. Lett.*, *34*, L14704, doi:10.1029/2007GL030221.

Shindell, D., and G. Faluvegi (2009), Climate response to regional radiative forcing during the 20th century, *Nat. Geosci.*, *2*, 294–300.

Shindell, D. T., H. Levy II, M. D. Schwarzkopf, L. W. Horowitz, J.-F. Lamarque, and G. Faluvegi (2008), Multi-model projections of climate change from short-lived emissions due to human activities, *J. Geophys. Res.*, *113*, D11109, doi:10.1029/2007JD009152.

Stier, P., J. Feichter, E. Roeckner, S. Kloster, and M. Esch (2006), The evolution of the global aerosol system in a transient climate simulation from 1860 to 2100, *Atmos. Chem. Phys.*, *6*, 3059–3076.

Takemura, T., Y. Tsushima, T. Yokohata, T. Nozawa, T. Nagashima, and T. Nakajima (2006), Time evolutions of various radiative forcings for the past 150 years estimated by a general circulation model, *Geophys. Res. Lett.*, *33*, L19705, doi:10.1029/2006GL026666.

Taylor, K. E., and J. E. Penner (1994), Response of the climate system to atmospheric aerosols and greenhouse gases, *Nature*, *369*, 734–737.

G. Faluvegi and D. Shindell, NASA Goddard Institute for Space Studies, 2880 Broadway, New York, NY 10025, USA. (drew.t.shindell@nasa.gov)

Y. Ming and V. Ramaswamy, NOAA Geophysical Fluid Dynamics Laboratory, 201 Forrestal Rd., Princeton, NJ 08540, USA.

M. Schulz, Laboratoire des Sciences du Climat et de l'Environnement, CEA/CNRS-IPSL, L'Orme des Merisiers, Bat 712, Point courier 132, F-91191 Gif-sur-Yvette, France.

T. Takemura, Research Institute for Applied Mechanics, Kyushu University, 6-1 Kasaga-koen, Kasuga, Fukuoka 816-8580, Japan.